Science of the Total Environment 846 (2022) 157395

Contents lists available at ScienceDirect

Science of the Total Environment

journal homepage: www.elsevier.com/locate/scitotenv

CO_2 adsorption on pyrolysis char from protein-containing livestock waste: How do proteins affect?

Noemí Gil-Lalaguna [a,b,*], África Navarro-Gil [a,b], Hans-Heinrich Carstensen [b,c], Joaquín Ruiz [a,b], Isabel Fonts [a,b], Jesús Ceamanos [a,b], María Benita Murillo [a,b], Gloria Gea [a,b]

[a] Engineering Research Institute of Aragón (I3A), University of Zaragoza, Mariano Esquillor St., 50018 Zaragoza, Spain
[b] Department of Chemical and Environmental Engineering, Engineering and Architecture School, University of Zaragoza, María de Luna St., 50018 Zaragoza, Spain
[c] Fundación Agencia Aragonesa para la Investigación y Desarrollo (ARAID), Mariano Esquillor St., 50018 Zaragoza, Spain

HIGHLIGHTS

- Chars from proteins and livestock waste adsorb CO_2 reversibly.
- Good fitting of micropore volume filling theory for CO_2 adsorption
- N-functionalities on pyrolysis chars surfaces do not benefit CO_2 uptake.
- Higher pyrolysis temperatures results in higher adsorption capacities of chars.
- The potential contribution of inorganics to CO_2 uptake should be further studied.

GRAPHICAL ABSTRACT

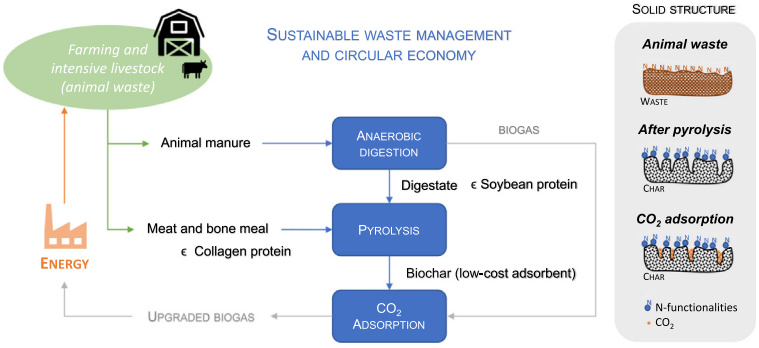

ARTICLE INFO

Guest Editor: Raffaello Cossu

Keywords:
Pyrolysis char
Proteins
Livestock wastes
CO_2 adsorption capacity
Ultra-microporosity
N-functionalities

ABSTRACT

Biogas generation through anaerobic digestion provides an interesting opportunity to valorize some types of animal waste materials whose management is increasingly complicated by legal and environmental restrictions. To successfully expand anaerobic digestion in livestock areas, operational issues such as digestate management must be addressed in an economical and environmentally sustainable way. Biogas upgrading is another necessary stage before intending it to add-value applications. The high concentration of CO_2 in biogas results in a reduced caloric value, so the removal of CO_2 would be beneficial for most end-users. The current work evaluates the CO_2 uptake properties (thermogravimetry study) of low-cost adsorbent materials produced from the animal wastes generated in the livestock area itself, specifically via pyrolysis of poorly biodegradable materials, such as meat and bone meal, and the digestate from manure anaerobic digestion. Therefore, the new element in this study with respect to other studies found in the literature related to biochar-based CO_2 adsorption performance is the presence of high content of pyrolyzed proteins in the adsorbent material. In this work, pyrolyzed chars from both meat and bone meal and co-digested manure have been proven to adsorb CO_2 reversibly, and also the chars produced from their representative pure proteins (collagen and soybean protein), which were evaluated as model compounds for a better understanding of the individual performance of proteins. The ultra-microporosity developed in the protein chars during pyrolysis seems to be the main explanation for such CO_2 uptake capacities, while neither the BET surface area nor N-functionalities on the char surface can properly explain the observed results. Although the CO_2 adsorption capacities of these pristine chars (6–41.0 mg CO_2/g char) are far away from data of commercially activated carbons (~80 mg CO_2/g char), this application opens a new via to integrate and valorize these wastes in the circular economy of the primary sector.

* Corresponding author at: Department of Chemical and Environmental Engineering, Engineering and Architecture School, University of Zaragoza, María de Luna St., 50018 Zaragoza, Spain.
E-mail address: noemigil@unizar.es (N. Gil-Lalaguna).

http://dx.doi.org/10.1016/j.scitotenv.2022.157395
Received 15 January 2022; Received in revised form 9 June 2022; Accepted 11 July 2022
Available online 14 July 2022

1. Introduction

The production of biogas is being actively promoted by the European Union within the European climate and energy framework program by 2030. This European framework aims to address environmental and economic issues regarding the reduction of greenhouse gas emissions, the management of high energy prices and EU dependence on energy imports, especially for oil and gas, as well as the upgrading of energy infrastructure by means of providing an attractive scenario for investors in new installations. In order to take these policies forward, the production of biogas appears as a source of renewable energy for heating, power and even for the transport sector (Document 52022SC0230 - EUR-Lex, 2020).

Biogas is the gaseous product resulting from the anaerobic digestion process of organic matter and is mainly composed of CH_4 (50 to 70 vol%) and CO_2 (30 to 50 vol%), as well as traces of H_2S and H_2 (Angelidaki et al., 2018). Owing to this composition, its calorific content is still more than half of that of natural gas (20–26 MJ/m^3_{STP}), so producing biogas from organic residues could be considered a way of energy recovery.

The installed capacity of biogas in the European Union is still relatively small, even though most countries possess a high production potential due to the huge generation of biodegradable wastes. In this sense, biogas generation is emerging in recent years in farming and intensive livestock areas, where significant amounts of animal and agricultural wastes suitable for anaerobic digestion or co-digestion are generated. However, the composition of farming and agricultural wastes is heterogeneous, each showing different degradation behaviour, so the variability of feedstock for the anaerobic digestion process is limited. For instance, manure is a suitable material for anaerobic digestion (Awe et al., 2017), while other animal waste materials, such as meat and bone meal (MBM), are poorly biodegradable, so other sustainable management ways must be implemented.

The use of livestock waste as fertilizer for nearby arable lands is a common practice in the primary sector. However, due to their environmental or sanitary impact, strict regulations are applied to these management routes. For instance, the Council Directive 91/676/EEC sets upper limits of 170 kg N/ha that can be applied annually in form of manure in those areas designated as vulnerable zones, which are those draining into waters that are or could be affected by high nitrate levels and eutrophication. In the case of MBM residues, they fall into three categories according to their risk of transmitting diseases to humans or animals: category 1 (Cat 1) for the highest risk materials, category 2 (Cat 2) for intermediate risk materials and category 3 (Cat 3) for the lowest risk materials. The existing legislation in the European Union prohibits the use of Cat 1 and imposes many restrictions on the use of Cat 2 and Cat 3 in the animal feed industry or as fertilizers (Regulation (EC) N° 1069/2009 of the European Parliament and of the Council). These uses of MBM need strict monitoring to ensure no mixture between residues from different categories. Sometimes traceability cannot be guaranteed, so the most severe restrictions should be applied. These limitations open the possibility of valorizing MBM residues via other management alternatives, such as pyrolysis.

Just like the original waste, the solid by-product from anaerobic digestion, called digestate, needs adequate management to avoid environmental problems. Therefore, the stage of anaerobic digestion is not enough for a complete management route of the entire range of livestock waste, but a more flexible and integrated process is needed. Such an integrated approach could combine the anaerobic digestion or co-digestion of manure with a pyrolysis stage that would convert the digestate, as well as other non-digestible residues such as MBM, to biochar. These types of biochar could be used for CO_2 removal in the upgrading process of biogas. The high concentration of CO_2 in biogas results in a reduced caloric value, so the removal of CO_2 would be beneficial for most end-users.

In this sense, this work focuses on the use of biochar produced from animal waste materials for the adsorption of CO_2 from biogas. Among current commercial technologies for biogas upgrading, activated carbon has been proven to be an effective adsorbent, but its relatively high price substantially increases the overall process costs and creates a severe burden for its implementation in the intensive livestock farming economy. Consequently, there is an increasing interest in identifying low-cost adsorbent materials (Mulu et al., 2021). The ability to use waste materials to produce such low-cost adsorbents would contribute to sustainable waste management and a circular economy.

Biochar is a carbon-rich porous material with high potential as an adsorbent material for the treatment of gaseous effluents. Even though non-negligible CO_2 adsorption capacities are reported in the literature for pristine chars produced from biomass carbonization (see Table 1), few studies focus on its direct application, but most studies focus on the production of CO_2 adsorbents following multistep processes, involving different physical and chemical activation stages (see Table 1). Some of these treatments significantly increase the CO_2 adsorption capacity, while others do not appear to be good enough to offset the extra cost of such activation stages.

Among those activation treatments, some of them, such as physical activation with CO_2 (Zhang et al., 2015) or chemical activation with KOH (Chen et al., 2017; Liu and Huang, 2018) enhance the development of highly ultra-microporous structures in biochar, thereby improving their CO_2 adsorption capacities. The CO_2 adsorption capacity of activated biochars can also be improved by the introduction of amine groups on the solid surface, whose basic character allows to chemically retain the acidic CO_2, which implies high values of heat requirements to be regenerated (90–150 kJ/mol) (Wang et al., 2017).

In the same way as the amine superficial groups, there is some experimental evidence that points to a beneficial effect of the nitrogen content (Liang et al., 2016; Liu and Huang, 2018; Saha et al., 2018) and the specific presence of pyrrolic and pyridinic groups (Liu and Huang, 2018; Wang et al., 2019). Quantum mechanical calculations show that pyridinic nitrogen incorporation induces an increased CO_2 adsorption strength (Jiao et al., 2014) and that, among the N-functionalities studied, pyridone and pyridine groups present the highest adsorption energies (-0.224 and -0.218 eV) because of their acid-base interactions with the CO_2 molecule. However, experimental results obtained by other studies contradict the positive effect of the nitrogen content (Xiong et al., 2013; Zhang et al., 2014) or do not firmly support the enhancing effect of pH (Sethupathi et al., 2017) or the presence of other N-containing functional groups different to the amine one (Chen et al., 2016; Karim Ghani et al., 2015; Madzaki et al., 2016).

Apart from the functionalization of biochar with N-containing groups, the direct use of protein-containing materials as feedstock for pyrolysis would yield biochar with a significant fraction of N-containing functional groups, mostly in the form of quaternary-N, pyridinic-N and pyrrolic-N (Leng et al., 2020). Therefore, to reduce the cost and time requirements of multistep procedures, the utilization of raw materials with high N-content, such as protein-rich animal wastes, to produce N-rich biochar might be a potential approach that deserves consideration and evaluation.

The literature on the adsorption properties of N-rich biochar produced from protein-rich animal wastes is scarce but highlights good adsorption results for the removal of Basic Red 9 dye (Côrtes et al., 2019), bisphenol A (Cai et al., 2021) and even CO_2 (see pig manure, sewage sludge and soybean stover in Table 1). Some studies in the literature point out that the CO_2 uptake properties of chars can also be enhanced by increasing the alkalinity of their surface (Dissanayake et al., 2020a). N-containing functional groups (such as amide, imide, pyridinic, pyrrolic and lactam groups) can contribute to the surface basicity and promote CO_2 adsorption on N-rich biochars (Qiao et al., 2020), but also the presence of alkali and alkaline earth metals can favor the formation of basic sites with a strong affinity for CO_2 or even involve chemical transformations to capture CO_2 in the form of carbonates (Xu et al., 2016). Therefore, livestock waste with high protein content and significant content of ash (rich in alkali and alkaline earth metals) could be considered potential precursors for low-cost CO_2 adsorbents. However, the presence of other macro-components in these wastes could influence the morphological structure and the surface chemistry of the biochar obtained. Therefore, evaluating the CO_2 adsorption mechanism on chars produced from the main pure proteins present in these animal wastes would be helpful to improve the understanding of the contribution of proteins and N-containing functional groups remaining on the biochar surface from these complex residues. Such a study needs to

Table 1
Literature results about CO_2 adsorption capacities of pristine and activated pyrolysis biochars.

Raw material	Pyrolysis temperature (°C)	Adsorption temperature (°C)	Adsorption capacity of pristine chars (mg CO_2/g)	Activation treatment	Adsorption capacity of activated chars (mg CO_2/g)	Reference
Pig manure	500	25	18.2	n.a.	–	(Xu et al., 2016)
Wheat straw			23			
Sewage sludge			34.4			
Sugarcane Bagasse	300, 450, 600	25	25–34	n.a.	–	(Creamer et al., 2014)
Hickory wood	300, 450, 600		33–48			
	300, 450, 600		52–74			
Perilla leaf	700	50 °C	101.7	n.a.	–	(Sethupathi et al., 2017)
Korean oak		** Biogas surrogate	26.3			
Japanese oak			16.7			
Soybean stover			31.1			
Coconut shell	800	30	46.4	Monoethanolamine impregnation	45.6	(Karim Ghani et al., 2015)
Coconut shell	500	25	66	Urea modification and KOH activation	61.6–211.2	(Chen et al., 2016)
	450		19.7		19.1	
Sawdust	750	30	45.2	Monoethanolamine impregnation	39.7	(Madzaki et al., 2016)
	850		47.5		44.8	
	500		27.8			
Walnut shell	700	30	56.1	Metal impregnated	67.6–80.0	(Lahijani et al., 2018)
	900		69.1			
Cottonwood	600	25	58.8	Pyrolysis with varying amounts of $AlCl_3$, $FeCl_3$ and $MgCl_2$	27–71	(Creamer et al., 2016)
Coffee grounds	400	35	6.16	Ammoxidation and KOH activation	18.0–117.5	(Liu and Huang, 2018)
Walnut shell	500	25	23.8	Low temperature through $NaNH_2$	74.8–134.6	(Yang et al., 2019)
Cotton stalk	600	20	58	Thermal treatment with NH_3/CO	56–100	(Xiong et al., 2013)
Cotton stalk	600	20	38	Thermal treatment with NH_3/CO	15–98	(Zhang et al., 2016)
Popcorn	800	20	~100	Thermal treatment with KOH	202.4	(Liang et al., 2016)

All adsorption tests shown in Table 1 were carried out with 100 vol% CO_2 and at atmospheric pressure, except the study marked with **, which used surrogate biogas composition [H_2S (0.3 vol%), CO_2 (40 vol%), and CH_4 (59.7 vol%)] under a relative humidity of 20 vol% and at atmospheric pressure.

include chars produced from both, the pure proteins and the original residues.

In the present work, the CO_2 adsorption capacities of chars produced by pyrolysis of two animal wastes, co-digested manure (CDM) and MBM, were investigated. When comparing MBM and CDM, the differences in the origin of the protein fractions should be considered. Collagen, as part of the skin and musculoskeletal system of the animals, is one of the major constituents of MBM, while soybean protein (a plant-based protein) is usually part of animal feeding, so remains of it can be found in the excrements and, in turn, in the CDM. The CO_2 adsorption capacities of the chars prepared from these two representative proteins were also investigated.

Hence, the specific objectives of this work are: (1) to determine the CO_2 adsorption isotherms (at 298 K) for the pyrolysis chars obtained from livestock waste and pure proteins; (2) to analyze the effect of pyrolysis temperature and char characteristics (textural properties, pH and N-functionalities) on the CO_2 adsorption capacity and (3) to test the reversibility of CO_2 adsorption after regeneration at increased temperature.

2. Experimental

2.1. Char production

Two protein-rich animal wastes, co-digested manure (CDM) and meat and bone meal (MBM), and two proteins, soybean protein (SP) and collagen protein (CP), were used as feedstock for char production via pyrolysis. The CDM (supplied by HTN Biogas Company, in Spain) was obtained from anaerobic co-digestion of cattle manure and agricultural residues, and subsequently separated in a decanter centrifuge; this digestate was oven-dried at 105 °C when received in our lab. The MBM (stabilized in an autoclave reactor with steam at 120 °C) was supplied by the Spanish company Residuos Aragón S.A. The two proteins, SP (with a stated protein content of 90 %) and CP, were commercial products acquired in a drugstore. The particle sizes of these materials were: (i) < 100 μm for SP and CP, (ii) < 150 μm for CDM and (iii) MBM particle size distribution between 100 and 400 μm (64 %) and > 400 μm (36 %).

Pyrolysis experiments were performed in a lab-scale fixed-bed plant of 2–3 g capacity. The fixed bed reactor, made of stainless steel, was placed inside an electrically heated oven that allowed the heating of the sample at a rate of 10 °C/min up to the final pyrolysis temperature (350, 550 or 750 °C), which was maintained for one hour. Previously measured temperature profiles confirmed that the temperature inside the reaction zone was constant within ±1 °C. A N_2 carrier gas flow of 50 mL_{STP}/min was used to ensure an inert atmosphere in the reactor and to remove volatile products. The yields of the solid products (shown in Table 2) were determined by the weight difference of the reactor tube before and after the experiment. The experimental variability was evaluated through 3 or 4 replicates at each pyrolysis temperature.

The different (a total of 12) char samples produced are named by a combination of letters related to the raw material used (CDM, MBM, SP or CP) followed by a number indicating the final pyrolysis temperature. For example, CDM350 refers to char prepared by pyrolysis of co-digested manure at 350 °C.

All char samples were crushed and sieved (25–63 μm size) before being characterized and used in the CO_2 adsorption tests.

2.2. Char characterization

Char samples obtained in the pyrolysis of the four materials were characterized in terms of chemical composition (elemental analysis), pH, surface chemistry (FTIR and XPS spectroscopy) and textural properties to explain the results observed for CO_2 adsorption capacities. The elemental analysis was performed with a LECO® CHN 628 Series Elemental Analyzer. For pH measurement, char was mixed with deionized water in a 20:1 water: char (mL:g) ratio for 1.5 h with stirring (Rajkovich et al., 2012); afterwards, pH was determined with an Orion model Star A215 pH meter. Functional groups located on the char surface were identified by Attenuated Total Reflection-Fourier Transform Infra-Red (ATR-FTIR) spectroscopy analysis, using an Agilent Cary 600 FTIR spectrometer, with a resolution of 4 cm^{-1} in the wavenumber range of 4000–400 cm^{-1} (medium IR region).

Table 2
Characterization results of raw materials and pyrolysis chars (wt%, wet basis).

	Char yield (wt%)	C (wt%, wet basis)	H (wt%, wet basis) [a]	N (wt%, wet basis)	Ash (wt%, wet basis) [b]	H/C molar ratio	N/C molar ratio	pH	N-functionalities identified by XPS (% atoms)		
									Pyridinic	Pyrrolic + Pyridonic	Pyridinic oxide
CDM	–	29.5 ± 0.5	4.1 ± 0.2	2.05 ± 0.09	37.4 ± 0.6	1.67	0.06	8.2 ± 0.1			
CDM350	61 ± 3	32.6	2.5	2.13	49.7	0.92	0.06	8.4	0.2	2.2	0.4
CDM550	52 ± 3	37	1.5	2.27	66.3	0.49	0.05	9.7	0.7	1.0	0.5
CDM750	42 ± 1	36.2	0.5	1.23	63.8	0.17	0.03	11	0	1.7	0
SP	–	48.88 ± 0.07	6.56 ± 0.01	13.63 ± 0.01	4.2 ± 0.7	1.61	0.24	6.7 ± 0.1			
SP350	40 ± 3	57.7 ± 2	4.9 ± 0.03	13.7 ± 0.9	10.5	1.02	0.20	9.1	2.7	8.0	0
SP550	27 ± 1	46 ± 2	2.6 ± 0.02	10.1 ± 0.1	15.6	0.68	0.19	9.8	3.9	5.8	0.8
SP750	25 ± 4	56 ± 0.8	1.3 ± 0.1	9.5 ± 0.1	16.8	0.28	0.15	10.0	1.9	7.0	0
MBM	–	46.07 ± 0.06	7.1 ± 0.2	10.7 ± 0.4	16.5 ± 0.2	1.85	0.20	6.2 ± 0.1			
MBM350	44 ± 3	41 ± 1	3.7 ± 0.3	8.4 ± 0.4	37.5	1.08	0.18	9.0	1.5	5.5	1.0
MBM550	30 ± 4	39 ± 0.9	1.5 ± 0.2	6.5 ± 0.1	55.0	0.46	0.14	10.0	1.1	3.4	0.9
MBM750	29 ± 3	36.4 ± 0.1	0.68 ± 0.01	4.9 ± 0.1	56.9	0.22	0.12	10.4	0.8	2.5	0.3
CP	–	44.2 ± 2	6.8 ± 0.2	16.9 ± 0.5	1.1 ± 0.1	1.85	0.33	6.1 ± 0.1			
CP350	36 ± 3	56.7 ± 0.7	4.5 ± 0.05	14.6 ± 0.2	3.1	0.95	0.22	8.0	2.9	6.2	0
CP550	25 ± 2	65 ± 1	2.6 ± 0.2	13.98 ± 0.05	4.4	0.48	0.18	8.4	4.2	5.8	0.5
CP750	19 ± 2	61 ± 3	1.2 ± 0.1	10.5 ± 0.5	5.8	0.24	0.15	10.1	4.5	2.6	0.7

[a] Hydrogen content includes hydrogen from moisture.
[b] The ash content in the raw materials and in CDM char was experimentally determined according to ISO-18122-2015 standard, while ash content for protein chars and MBM chars were calculated assuming that the ash contained in the raw material does not devolatilize during pyrolysis. This assumption is not valid for CDM, as its carbonate fraction is expected to be devolatilized during the thermal process, especially at 750 °C.

The N-containing functional groups at the external surface layer of the char samples were characterized by X-ray Photoelectron Spectroscopy (XPS) using a Kratos AXIS Supra XPS spectrometer with a monochromatic Al Kα X-ray source (photon energy: 1486.6 eV). Curve fitting of N 1 s data was performed with version 2.3.15 of CasaXPS software. The binding energy scale was set to a value of 284.9 eV for the graphitic carbon C 1 s peak. The N 1 s spectra of the raw materials and char samples were deconvoluted in peaks around different binding energies (BE).

Textural properties of chars were investigated using a Quantachrome Autosorb® 6 Surface Area and Pore Size Analyzer. The samples were firstly degassed at 523 K in vacuum for 8 h to remove any adsorbed molecules from the pores. N_2 adsorption and desorption isotherms were recorded at 77 K for the relative pressure (P/P_o) range of 0.01–0.99 and the data were used to extract the BET surface area. The N_2 data were complemented with CO_2 adsorption measurements at 273 K for the P/P_o range of 0.0003–0.03. Latter data are more sensitive to very small micropores than the N_2 results (Jagiello et al., 2019; Wedler and Span, 2021). Both types of isotherms were analyzed using the Dubinin-Radushkevich (DR) equation and non-local density functional theory (NLDFT) to determine the micropore volume and the pore size distribution, respectively.

2.3. CO_2 adsorption procedure

The CO_2 adsorption capacities of the char samples were examined by thermogravimetric analysis (TGA) with a Netzsch STA 449 Jupiter® thermobalance. The adsorption tests were done at 298 K and atmospheric pressure. About 50 mg of ground and sieved char sample (25–63 μm size) was first degassed at 250 °C for one hour in a N_2 stream (100 mL_{STP}/min). After cooling to 298 K, the char sample was exposed to various CO_2/N_2 mixtures, with a CO_2 volume fraction ranging from 2 % to 83 % (relative pressure range of 0.0003–0.013). The use of 20 mL_{STP}/min of N_2 as protective gas flow in the TGA apparatus prevented the study of pure CO_2 adsorption.

The char was exposed to each concentration of CO_2 for 50 min to allow equilibrium between the gas phase and surface adsorption. The CO_2 adsorption capacity of chars (mg CO_2/g char) for each CO_2 partial pressure was calculated from the sample weight gain relative to the weight in a pure N_2 atmosphere (N_2 adsorption on char samples was considered negligible). In some cases, the sample weight was still slightly increasing after 50 min, hence the equilibrium CO_2 adsorption capacities could be somewhat higher than those reported here.

Once adsorption tests for a preselected set of partial CO_2 pressures were done, the CO_2 flow was replaced by N_2 and the temperature was increased to 150 °C. This leads to CO_2 desorption if the adsorption process is reversible. The mass loss occurring when increasing the temperature indicates how reversible the adsorption process is. Once this test was completed, another set of adsorption measurements was carried out. Three such desorption tests were incorporated into the adsorption tests.

3. Results and discussion

3.1. Char characterization

Char samples obtained in the pyrolysis of the four materials were characterized in terms of chemical composition (elemental analysis), pH, surface chemistry (FTIR and XPS spectroscopy) and textural properties to explain the results observed for CO_2 adsorption capacities and evaluate the effect of pyrolysis temperature and type of char precursor.

3.1.1. Elemental composition

The elemental analyses of the chars produced from the animal wastes and from their representative proteins show significant differences (Table 2). Chars from the proteins are much richer in C and N than chars from the animal residues. This is explained by differences in the ash content. The ash content in the original wastes (determined at 550 °C according to ISO-18122-2015 standard) is as high as 16 wt% in raw MBM and 37 wt% in CDM, while it is only 1 wt% in CP and 4 wt% in SP. Although a part of the inorganic fraction in the raw materials is expected to decompose during pyrolysis at the highest temperature (especially carbonates), the remaining amount of ash in the chars from the animal wastes still affects the final content of C and N, provoking a dilution effect.

After pyrolysis, chars are richer in C content than their original raw materials, except for MBM, which points to the occurrence of fewer condensation reactions during the process. Regarding N content, it is reduced in the solids after pyrolysis, except in the case of CDM. This seems to indicate the presence of more recalcitrant N-functionalities, for example in the form of heterocyclic structures. On the other hand, the loss of N at the lowest pyrolysis temperature is more obvious for CP than for SP.

The N/C ratios are higher in the protein-derived chars than in the waste chars, especially when they are compared to the CDM chars. Furthermore, the N/C molar ratios in CDM chars are 3–4 times lower than in MBM chars. This is related to the raw material composition, as CDM contains, apart

from proteins, a greater proportion of other macro-components rich in C, such as cellulose and lignin from agricultural residues.

Even though the C content does not follow a clear trend with pyrolysis temperature, a clear reduction in N content and a slight decrease in the N/C ratio with increasing pyrolysis temperature are observed for all materials. Similar declines are, in general, noticeable for H/C ratio. An increase in the pyrolysis temperature favors the loss of H-rich volatile organic matter, but also dehydrogenation and deoxygenation reactions, leading to a more hydrophobic char (less polar and with greater aromaticity). Biochar with hydrophobic and nonpolar characteristics may facilitate the CO_2 adsorption capacity by limiting the competition of H_2O molecules (Dissanayake et al., 2020b).

3.1.2. Surface chemical composition

As commented before, increasing the alkalinity of char surface could be beneficial for CO_2 adsorption. All the char samples analyzed in this work are alkaline regardless of the final pyrolysis temperature and feedstock used (pH values shown in Table 2). The alkalinity of the chars obtained is due to the presence of N-containing functional groups, which are present in both the residues and their representative protein chars, but also due to the high content in alkali and alkaline earth metals in the case of the residues chars. The pH values of the char samples (> 8 in all cases) increase with the final pyrolysis temperature, reaching values equal to or higher than 10 for chars obtained at 750 °C.

The nature of the functional groups present on the surfaces of the protein and livestock waste chars has been analyzed by ATR-FTIR (Fig. 1). When comparing the raw materials, it can be seen that the signal of OH groups (3400–3200 cm^{-1}) is significantly lower in CDM than in SP (chosen as its representative protein fraction). This means that proteins contribute more to surface OH groups than other macro-components of CDM. Both materials show a peak around 3250 cm^{-1}, corresponding to N—H vibrations, which could be ascribed to the amino group (peptide bond) in proteins and from the conformation of the polypeptide backbone. As expected, the intensity of this band in SP is significantly higher than in CDM. The amide group and the β sheet secondary structure of proteins (stretched segments of the polypeptide chain kept together by a network of hydrogen bonds between adjacent strands) are represented by the marked peaks around 1520 and 1625 cm^{-1}, which are significantly more prominent in the SP spectra than in CDM. The wide peak around 1387 cm^{-1} in the CDM spectrum could correspond with $CaCO_3$, which is usually added to animal feeding to improve the digestion process.

Unlike SP and CDM, the spectra of MBM and its representative protein (CP) are remarkably similar. The aforementioned bands (3250, 1520 and 1625 cm^{-1}) belonging to amide bonds and to the β sheet structure of proteins, which were noticeable in the spectrum of SP, are also evident in the spectra of CP and MBM. The most significant difference is the presence of two very strong bands in the MBM spectrum at 2915 and 2845 cm^{-1}, which can be assigned to -CH_2- groups, which are highly abundant in fatty compounds (mostly triglycerides and fatty acids) present in MBM.

Pyrolysis destroys most of the initial surface functional groups as can be observed by comparing the spectra obtained for the chars with those of the original feedstocks. No peaks related to OH-groups (3400–3200 cm^{-1}) are found in the spectra of the chars, except for the chars obtained from CP at 350 °C. The expected peak assigned to the amino group (N—H) at about 3250 cm^{-1} is not found either in any of the char spectra, which points to its destruction during pyrolysis. The peaks around 1625 and 1520 cm^{-1} represent the amide groups and appear in chars obtained from proteins and to a lesser extent in the low-temperature char from MBM. Chars from CP are found to contain the highest amounts of nitrogen functionalities and chars from CDM are those with the lowest amounts.

According to XPS analysis, N in the raw materials is found to be in the form of amide-N (BE = 400.1 ± 0.1 eV), amine-N (401.0 ± 0.2 eV), and, only in the case of MBM, a peak around 402.7 eV is observed, which could be attributed to N in nitrogenous bases of nucleotides. On the other hand, N in the char samples is found to be taking part of pyridinic-N (BE = 398.8 ± 0.2 eV), pyrrolic-N and pyridonic-N, which are quantified jointly due to the matching of their binding energies (BE = 400.7 ± 0.4 eV) (Pels et al., 1995) and pyridinic-N oxide (BE = 403.5 ± 0.3 eV). Table 2

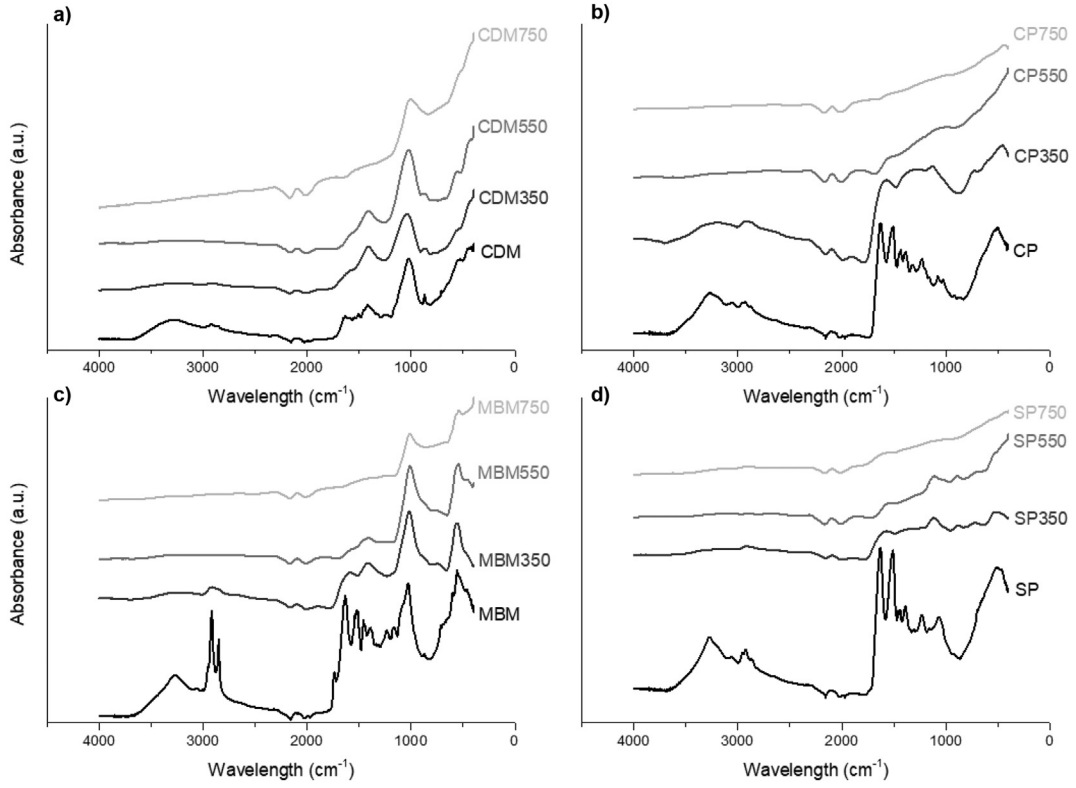

Fig. 1. FTIR spectra for the raw materials and chars obtained at the three different pyrolysis temperatures: a) Co-digested manure. b) Collagen protein. c) Meat and bone meal. d) Soybean protein.

shows the atomic fraction (%) of each of this N-group found on the chars surfaces with respect to the total identified atoms (C, O, N, S, Ca, Cl, Mg, Na, P, I and Al). Pyridinic-N and pyrrolic-N + pyridonic-N are the main N-containing groups found in chars, the latter group being the most abundant group regardless of the pyrolysis temperature. Moreover, the presence of these N-functionalities is more significant in the pure protein chars. The results also show a decrease in the presence of pyrrolic-N + pyridonic-N with the pyrolysis temperature, but not a clear trend for the pyridinic-N group.

As the pH values of the chars were found to increase with the pyrolysis temperature, it can be stated that the presence of these N-containing groups on its own does not explain the basic character of the chars, but this could be related to the mineral content, especially in the case of the animal waste chars.

3.1.3. Surface area and pore size

Fig. 2 shows some representative N_2 adsorption isotherms measured for the chars produced at 750 °C from all feedstocks. The data were taken with the standard setting, meaning that the P/P_o range is 0.01 to 0.99. This procedure does not return complete isotherms but only the high P/P_o part. Note the difference in Y-axis scales for protein-derived chars and waste-derived chars, which shows that the volumes of N_2 adsorbed by chars from the animal wastes (Fig. 2a and c) are much higher than those adsorbed by chars from the proteins (Fig. 2b and d).

Proteins, unlike other macro-components in biomass, are known to melt during thermal treatment (Hayashi et al., 1993), so it is a key factor that determines the final structure of the produced chars. The isotherms clearly show that N_2 adsorption at 77 K hardly takes place in protein chars (the cumulative volume of adsorbed N_2 hardly reaches 1 cm^3/g in most cases). This indicates a lack of macropores, mesopores or wider micropores. These results alone are insufficient to determine if these chars are good sorbent materials, because they are not sensitive to small micropores. As shown below, supplemental CO_2 adsorption isotherms are needed to fully analyze the textural properties.

Even though the lower parts of the isotherms ($P/P_o < 0.01$) are missing, the isotherms of the char wastes should be categorized as Type IVa according to IUPAC classification (Thommes et al., 2015), as they show pronounced hysteresis loops (adsorption and/or desorption branches are not in equilibrium). Carbonaceous adsorbents are usually described as Type I isotherms (Thommes et al., 2015), which suggests that the chars produced in this study differ in their textural properties from typical carbonaceous material. In the case of a Type IVa isotherm, capillary condensation is accompanied by hysteresis. This occurs when the pore width exceeds a certain critical value, which depends on the adsorption system and temperature. For instance, for N_2 adsorption in cylindrical pores at 77 K, hysteresis starts to occur for pores wider than ~ 4 nm (Thommes et al., 2015).

The multi-point BET analysis has been applied to the N_2 adsorption data to extract the BET surface areas (S_{BET}). The results are summarized in Table 3. As expected from the isotherms, the chars derived from the protein components (SP and CP) have small values of BET surface area, while higher areas are found for some of the chars from CDM and MBM. In any case, all values are far below the surface areas usually reported for commercially activated carbons (500–1500 m^2/g). The S_{BET} of CDM chars is positively affected by the pyrolysis temperature, while in the case of MBM chars such a positive effect is not noticeable when increasing the pyrolysis temperature from 550 to 750 °C.

The BET surface area of a non-porous, macroporous or mesoporous solid can be regarded as the effective area available for the surface adsorption of the specified adsorptive. However, if adsorption mainly occurs in micropores by filling the available pore volume, then this process is

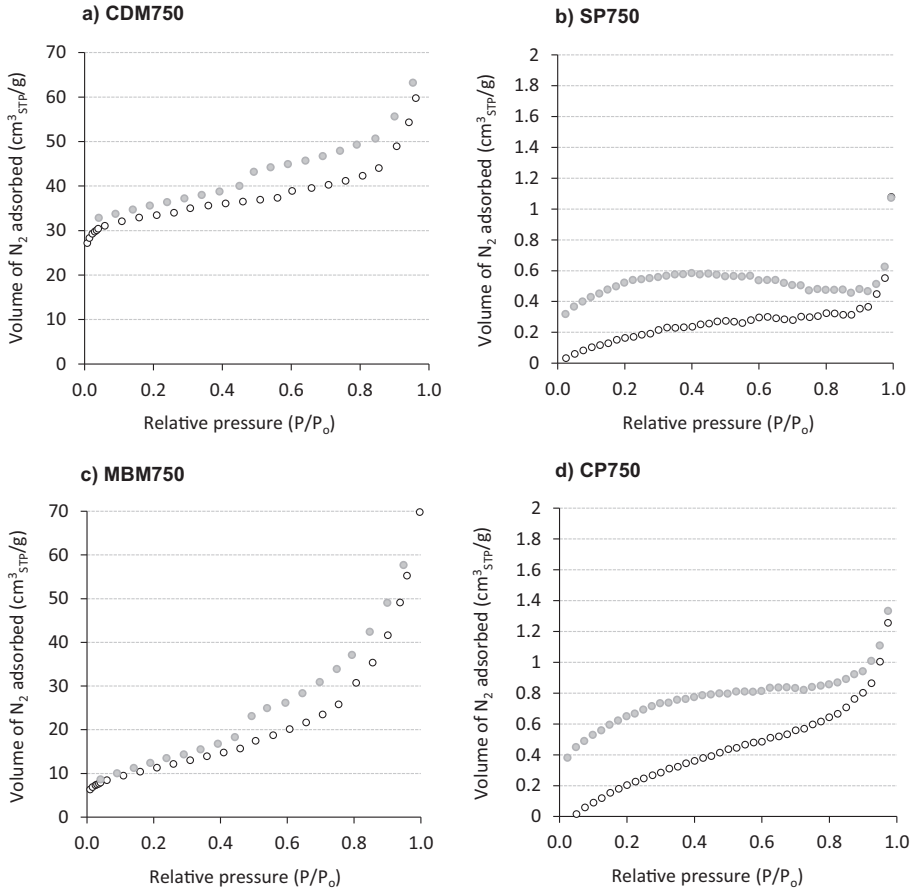

Fig. 2. N_2 adsorption isotherms (adsorption/desorption branches) of chars prepared at 750 °C from all feedstocks (open symbols represent the adsorption branch and closed symbols the desorption branch).

Table 3
Textural properties of chars determined from N_2 adsorption at 77 K and CO_2 adsorption at 273 K.

	N_2 adsorption at 77 K		CO_2 adsorption at 273 K	
	S_{BET} (m^2/g)	$V_{micropores}$ (cm^3/g)	$V_{micropores}$ (cm^3/g)	Average micropore width (nm)
CDM350	5	0.002	0.027	0.86
CDM550	29	0.012	0.048	0.71
CDM750	130	0.051	0.064	0.75
SP350	5	0.001	0.052	1.01
SP550	5	0.002	0.088	0.75
SP750	< 1	0.000	–	0.72
MBM350	15	0.004	0.034	0.94
MBM550	42	0.016	0.060	0.71
MBM750	40	0.014	0.037	0.75
CP350	13	0.003	0.042	0.99
CP550	< 1	0.000	0.108	0.76
CP750	1	0.001	0.094	0.72

distinctly different from the concept of surface coverage. Latter takes place largely on the walls of open macropores or mesopores (Thommes et al., 2015). Therefore, in the case of micropore filling, the interpretation of the adsorption isotherm only in terms of surface coverage is not correct.

It is well established that micropores play an important role in the CO_2 adsorption process occurring on activated carbons (Stoeckli, 1990; Wedler and Span, 2021). Therefore, applying the Dubinin-Radushkevich (DR) equation (Dubinin, 1989) to the adsorption data obtained for our chars at low P/P_o could give interesting information. This analysis should provide the volume of micropores that are involved in N_2 adsorption at 77 K. The results show that the protein chars provide little micropore volume for N_2 adsorption, while a clearly larger volume is available in the chars from animal waste. As with the S_{BET}, an increase of pyrolysis temperature results in a larger micropore volume in the waste chars that is available for N_2 adsorption. MBM550 and MBM750 are an exception to this as both provide quite similar volumes.

The application of non-local density functional theory (NLDFT) to N_2 adsorption isotherms of waste-derived chars reveals that N_2 adsorption occurs in micropores (< 2 nm size) and small mesopores (2–5.5 nm size). Fig. 3 shows the pore area distribution found for the waste-derived chars produced at the lowest and highest pyrolysis temperature when using NLDFT with a slit pore model. Note that the slit pore model reproduces the results for the chars produced at 750 °C (fitting error of 0.7 % for CDM750 and 1.5 % for MBM750, with reasonably good fitting across the whole range of P/P_o) much better than for those produced at 350 °C (fitting error of 5.3 % for CDM350 and 4.6 % for MBM350, with deviation especially noticeable at $P/P_o < 0.04$). From these results, one can again state that the increase in pyrolysis temperature favors the development of microporosity, especially in CDM chars. Hence, according to the NLDFT method, the micropore area in MBM350 and CDM350 accounts for 14 % of surface area, while it increases up to 38 % and 90 % in MBM750 and CDM750, respectively.

For the analysis of the narrowest microporosity (< 0.7 nm, denoted as ultra-micropores), CO_2 adsorption at 273 K was tested for all char samples. The linearization of the DR-equation (using an affinity coefficient of 0.33) properly reproduces the experimental data with correlation coefficients >0.999 in all cases. This shows that CO_2 adsorption by the chars produced in this study is well described by the theory of volume filling of micropores (TVFM) (Dubinin, 1989). The micropore volumes and average pore width obtained with the DR-method are summarized in Table 3. The micropore volume measured with CO_2 at 273 K shows a maximum value at the intermediate pyrolysis temperature (550 °C), except for CDM chars, for which an increase with temperature is observed. Therefore, too high pyrolysis temperature (750 °C) seems to negatively affect the ultra-micropore structure of proteins but could be favorable for the development of narrow micropores in other types of macro-components present in CDM, such as lignin or cellulose. In any case, all chars obtained at the lowest pyrolysis temperature (350 °C) show the highest average micropore width (reported by DR-method), which means that this temperature is too low for creating a good ultra-microporous structure. The impact of temperature on the average micropore width is more prone in the protein chars.

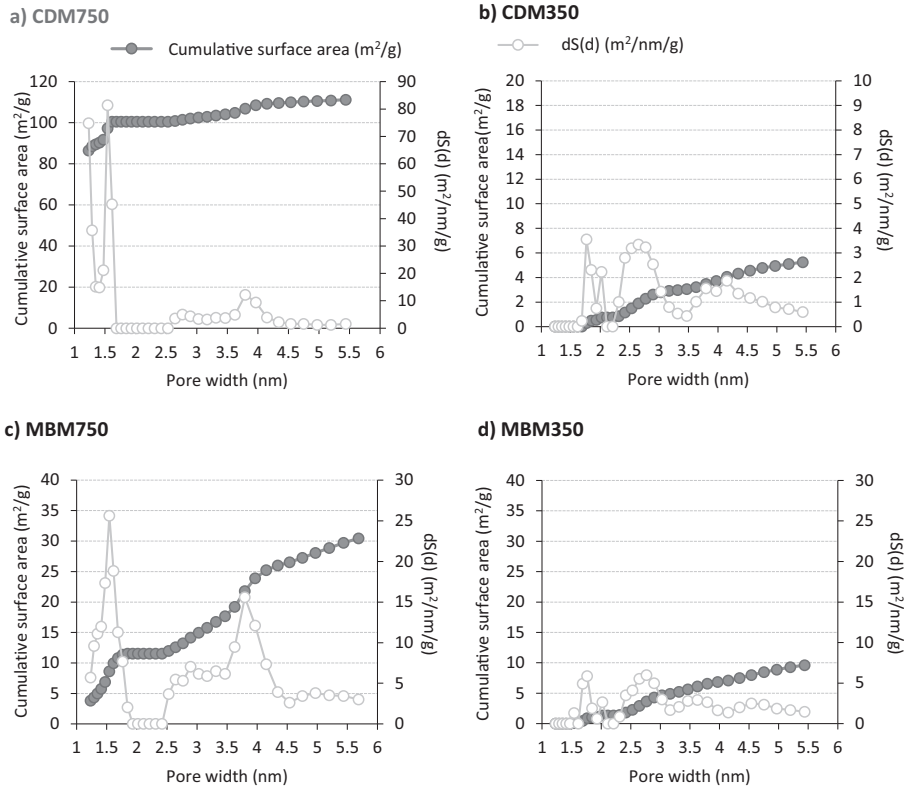

Fig. 3. Pore area distribution in CDM750, CDM350, MBM750 and MBM350 according to NLDFT model applied to N_2 adsorption isotherms at 77 K (slit pores).

Fig. 4 shows the micropore volume distribution in the chars produced at 550 °C, calculated according to the NLDFT model applied to the CO_2 adsorption data at 273 K. Only micropore width varying from 0.3 to 1.5 nm are considered. The NLDFT size distribution shows that the contribution of ultra-micropores (< 0.7 nm) to the total cumulative pore volume is slightly higher for protein chars than for waste chars: 68 % for CDM550 and 71 % for SP550, and 71 % for MBM550 and 74 % for CP550. Regarding the micropore volumes measured with CO_2 at 273 K, both the DR-method and the NLDFT calculations show higher values for the protein-derived chars than for waste-derived chars. The higher ash content in the waste-derived chars could explain these results.

3.2. CO_2 uptake properties

The CO_2 adsorption performance of the char samples was also examined by thermogravimetry at a more practical operation temperature for biogas cleaning (298 K instead of 273 K). The adsorption capacities for each sorbent material can be related to its weight gain during the process.

Fig. 5 shows the experimental CO_2 adsorption isotherms measured at 298 K. Interestingly, most of the profiles are well represented by Langmuir isotherms, which is a well-known surface area-based model. However, such an interpretation contradicts the analysis of the N_2 isotherms presented above, especially for protein chars that hardly contain S_{BET}. In fact, protein chars, which show lower S_{BET} than animal waste chars (Table 3), adsorb more CO_2 than their related livestock chars over the whole range of P/P_o. Hence, no direct relationship between S_{BET} and CO_2 adsorption is confirmed, which could indicate that CO_2 adsorption, under the operating conditions analyzed in this work, is not related to the surface coverage on the walls of macropores or mesopores.

According to Dubinin and coworkers, micropore adsorption on carbonaceous material can be well described by the theory of volume filling of micropores (TVFM) (Dubinin, 1989). To test if this theory also explains the current data, the results shown in Fig. 5 are replotted as Dubinin-Radushkevich (DR) plots in Fig. 6. The adsorption data for all chars follow straight lines with very similar slopes. The slopes correlate with the adsorption enthalpies and pore properties while the offsets are related to the adsorption volume at $P/P_o = 1$ (that is, the total available volume of micropores). The good linearity over the entire pressure range is consistent with the micropore volume filling model for CO_2 adsorption. This means that for the operational conditions used (298 K and P/P_o up to 0.013) dominantly micropores are responsible for CO_2 adsorption. A deviation from linearity in a DR plot would indicate that non-microporous surface areas contribute notably to the adsorption (Scarlat et al., 2018), but this is not the case here.

The total volume of micropores available in each char (measured with CO_2 at 298 K) is summarized in Table 4. These data differ from the volumes measured with CO_2 at 273 K (Table 3). As expected, larger volumes are observed at 273 K than at 298 K since a wider distribution of pore size becomes effective for physisorption at lower temperatures.

In general, the larger micropore volume (Table 4) and the higher contribution of ultra-micropores to the total cumulative pore volume (Fig. 4) in protein chars compared to animal waste chars could explain the higher CO_2 adsorption capacities found for protein chars, supporting the idea of micropore volume filling as the main mechanism of CO_2 physisorption on this type of chars.

A summary of the CO_2 uptake data obtained at 298 K for all the chars at the highest concentration of CO_2 in the gas (83 vol%) is plotted in Fig. 7. Better CO_2 adsorption performance of protein chars is clearly observed if compared to their related livestock waste chars. The higher ash content in the animal waste chars could explain their lower adsorption capacities. Other studies in the literature (Xu et al., 2016) state that char mineral fraction contributes to the chemical sorption of CO_2 via the mineralogical reactions, especially at adsorption temperatures higher than 298 K and for char with high moisture content. CDM and MBM chars contain non-negligible amounts of alkali (Na, K) and alkaline earth metals (Ca, Mg) that, in the presence of moisture, could react with CO_2 to form carbonate and bicarbonate. However, considering that the moisture content in the chars analyzed in this study is almost negligible and CO_2 adsorption temperature is 298 K, chemical sorption related to the minerals contained in the chars could contribute to CO_2 adsorption, but to a much lesser extent than physical sorption. Furthermore, despite the lower ash contents found in the chars produced from CP, their slope values in the DR-plot are quite similar to those obtained for the other materials (Fig. 6), thus pointing to similar

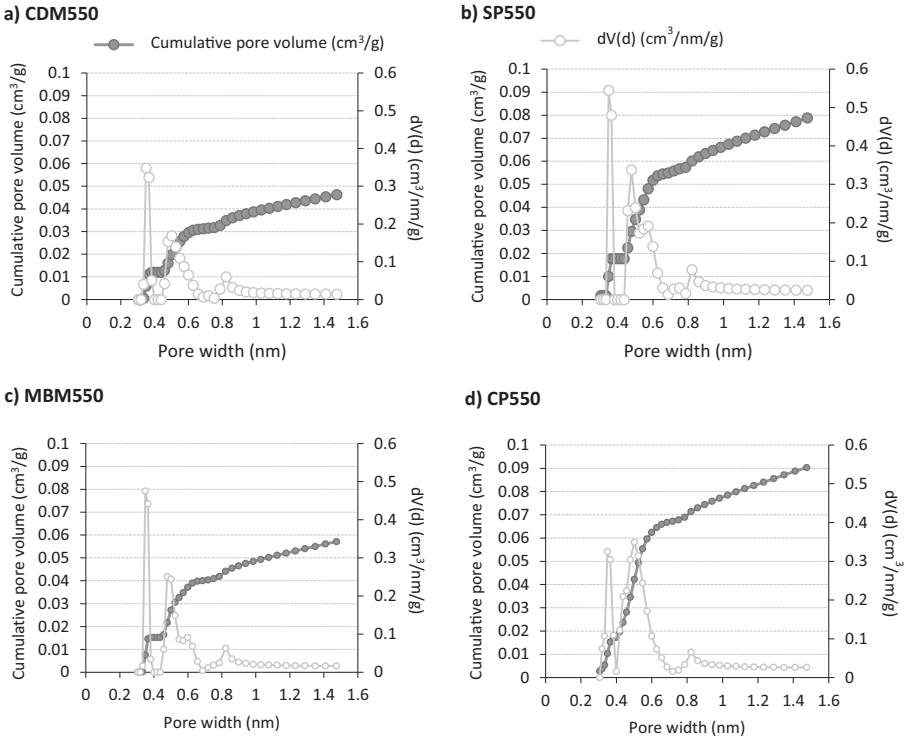

Fig. 4. Pore volume distribution in chars produced at 550 °C according to NLDFT model applied to CO_2 adsorption isotherms at 273 K.

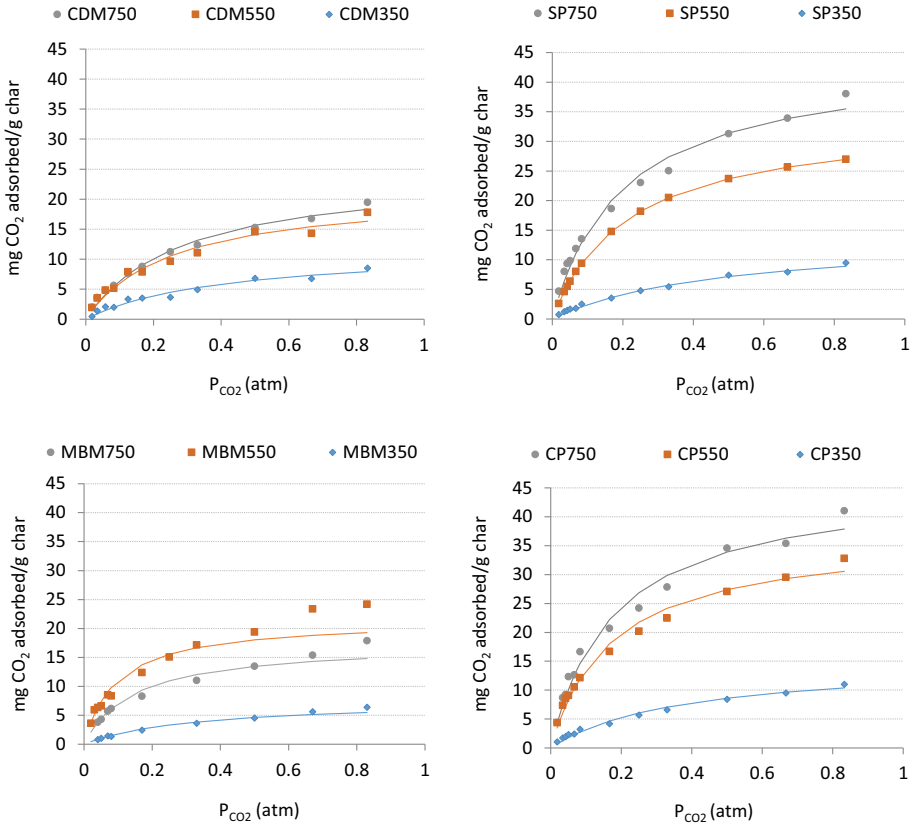

Fig. 5. Experimental CO_2 adsorption isotherms at 298 K (adsorption branch in TG analysis) and Langmuir fits for all char samples.

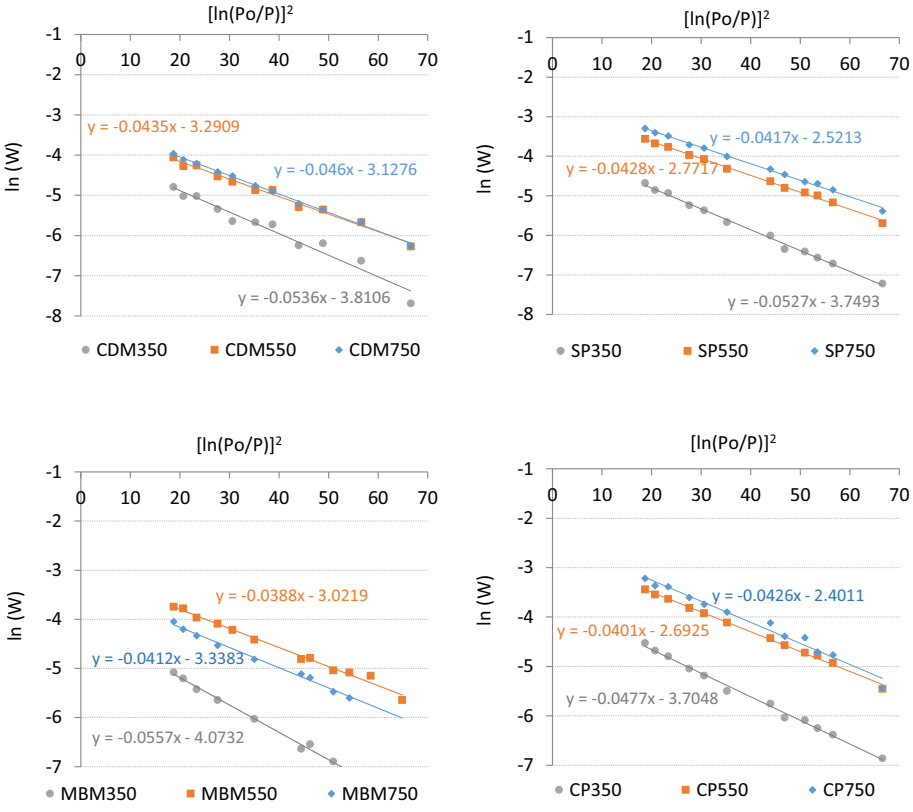

Fig. 6. DR plots of data previously shown in Fig. 5 (W is the volume of CO_2 adsorbed at each relative pressure P/P_o).

Table 4
Volume of micropores measured with CO_2 adsorption isotherms at 298 K.

	$V_{micropore}$ (CO_2_298 K) (cm^3/g)
CDM350	0.022
CDM550	0.037
CDM750	0.044
SP350	0.024
SP550	0.063
SP750	0.080
MBM350	0.017
MBM550	0.048
MBM750	0.035
CP350	0.025
CP550	0.068
CP750	0.091

adsorption energies regardless of the raw material. This also supports the idea that the contribution of minerals to chemisorption of CO_2 is expected to be small in these livestock waste chars.

If expressing the results on an ash-free basis, CO_2 adsorption capacities of chars from animal waste become greater than those for their representative protein chars (53 mg CO_2/g organic CDM550 vs. 34 mg CO_2/g organic SP550, and 54 mg CO_2/g organic MBM550 vs. 34 mg CO_2/g organic CP550). However, this difference is not as significant as it could be expected by considering the dilution effect of the inorganic content. This analysis seems to indicate that: (i) the carbonization of other organic macrocomponents (different from proteins) which are present in the livestock waste leads to a pyrolysis char with improved CO_2 uptake properties and/or (ii) during pyrolysis occurs any interaction between the organic and the inorganic fractions that results in a synergetic effect on CO_2 adsorption capacities. Future work focused on interaction effects between macrocomponents could help to elucidate this issue.

As can be seen in Fig. 7, pyrolysis temperature has a positive effect on the CO_2 adsorption capacities, except for chars obtained from MBM, for which the maximum is found at the intermediate pyrolysis temperature (550 °C). CO_2 adsorption capacities of protein chars prepared at 750 °C are essentially twice that of their related wastes (40 vs. 20 mg CO_2/g char), while these differences are, in general, less significant for the chars prepared at lower pyrolysis temperatures. This means that an increase of the pyrolysis temperature mainly improves the CO_2 uptake properties (at 298 K) of the two studied protein chars, while the impact of pyrolysis temperature on the waste chars is smaller. This positive effect of the pyrolysis temperature on the CO_2 adsorption capacities of the chars points out that the presence of N-functionalities on the char surface does not really benefit the CO_2 adsorption process, as increasing the pyrolysis temperature implies a loss of these functionalities (Fig. 1), specifically pyrrolic-N + pyridonic-N (Table 2). As commented in the introduction section, several authors have demonstrated the enhancement of CO_2 adsorption performance with the presence of amine groups on the char surface (Wang et al., 2017). However, in this work, pyrolysis of animal wastes and proteins have destroyed the amine groups that could be present in the raw materials, leading to chars with limited N-functionalities different from amines, such as pyridinic-N, pyrrolic-N and/or pyridonic-N, and pyridinic-N oxide (Table 2). Thus, this work does not report any evidence that the presence of those N-functionalities remaining on the char surface after pyrolysis of protein-containing feedstocks could improve the CO_2 adsorption capacity of these materials. Therefore, the improvement of CO_2 uptake properties of chars with the pyrolysis temperature (except for MBM550 and MBM750) might be related to an increase in the microporosity of the materials, as shown in Fig. 3, rather than an alteration in the surface nitrogen chemistry. The physical nature of CO_2 adsorption is also supported by the fact that all linear DR-plots show similar and small slope values (which are related to the free adsorption energies) regardless of the pyrolysis temperatures and even the raw material (Fig. 6).

The CO_2 adsorption results obtained in this work at 298 K for the highest concentration of CO_2 in the gas (83 vol%) show an acceptable linear correlation with the micropore volume determined at 273 K, as can be observed in Fig. 8.

As well as CO_2 uptake, the pH values of the chars increase with the pyrolysis temperature indicating that the evolution of the char alkalinity would be related to the enrichment of the mineral fraction rather than the presence of N-functionalities. In the case of CDM, higher pyrolysis temperatures can promote the thermal decomposition of the carbonates present in the raw material, thus increasing the concentration of metal oxides such as CaO or MgO, which have a more basic character than carbonates, which could enhance the capture of the acidic CO_2. Given that previous studies in the literature point out that the mineral fraction could contribute to the CO_2 sorption, the mineral enrichment of char with pyrolysis temperature (or transformation of it to more basic structures) could enhance chemical sorption to some extent. Therefore, as already mentioned above, a further study focused on the interaction between organic and inorganic fractions is recommended.

The CO_2 adsorption capacities obtained in this study for animal waste chars and their representative protein chars are in the same order of magnitude as those obtained for other lignocellulosic chars (such as chars from wheat straw or sugarcane) and for chars from N-rich waste (such as sewage

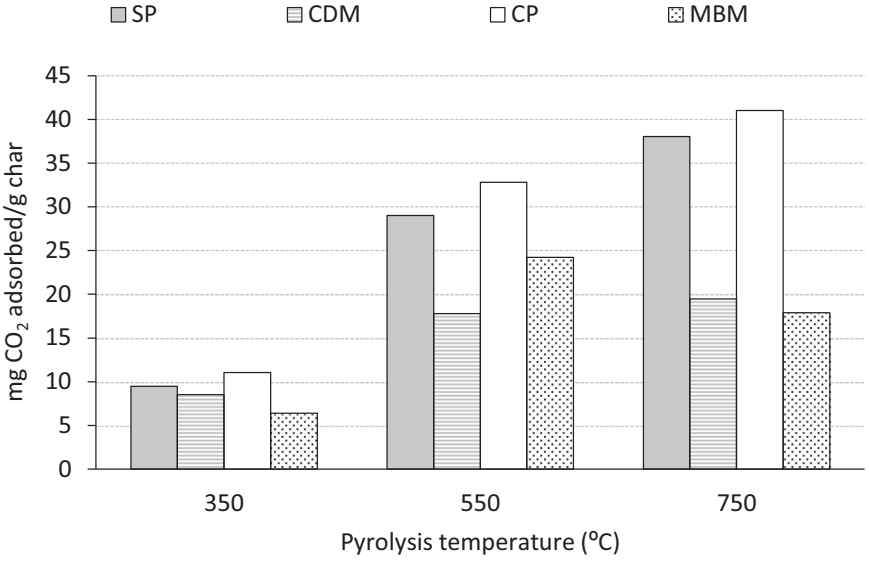

Fig. 7. CO_2 uptake at 298 K of all char samples (gas mixture with 83 vol% CO_2).

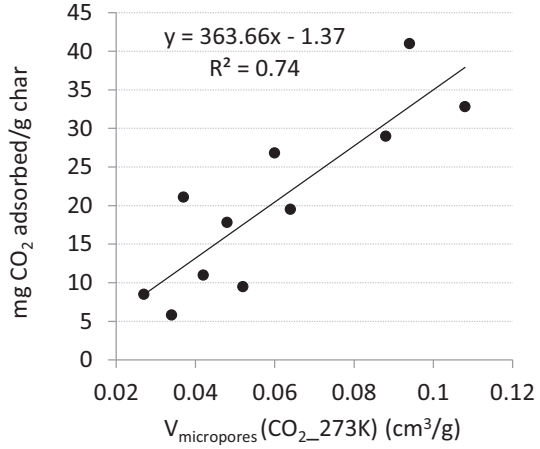

Fig. 8. Correlation of CO_2 uptake of all char samples at 298 K with the volume of micropores determined at 273 K with the DR-method.

sludge), but are poorer if compared with some data from functionalized or activated chars (see Table 1). These results suggest that pristine chars from animal wastes could be considered as potentially low-cost adsorbents to assist in biogas upgrading on the same livestock facilities where they have been generated.

3.3. Regeneration of char after CO_2 adsorption

Table 5 summarizes the CO_2 uptake results (obtained at the highest concentration of CO_2 of 83 %) for chars after successive adsorption-regeneration cycles. A slight loss of CO_2 adsorption capacity was observed between cycles #1 and #2 (loss between 1 % and 24 % in the case of animal waste chars and 2–5 % for protein chars), while more stable CO_2 uptakes are observed for cycles #2 and #3. These preliminary results suggest that CO_2 adsorption occurring in these chars is a reversible process, but also show that a first step of char stabilization occurs, especially in those chars derived from animal waste. More work is required to confirm this observation.

This apparent reversibility of the process supports the idea that the contribution of CO_2 chemical sorption through the precipitation with minerals contained in the livestock waste chars plays a secondary role since chemical sorption conserves CO_2 in a more stable chemical form compared to that through physical sorption (Xu et al., 2016). In any case, further analysis is required to confirm this hypothesis.

In summary, given that: (i) higher contents of nitrogen and N-functionalities on char surface cannot be clearly related to increased CO_2 adsorption capacities, (ii) the theory of volume filling of micropores describes well the experimental data of CO_2 uptake and (iii) CO_2 adsorption process seems to be reversible to a large extent, it can be stated that both protein chars and animal waste chars mainly adsorb CO_2 through physisorption process which is positively related to the development of very small micropores.

Table 5
Cyclic adsorption-desorption behaviour of char samples (mg CO_2/g char adsorbed at the highest CO_2 concentration).

	Cycle #1	Cycle #2	Cycle #3
CDM350	8.5	7.4	7.8
CDM550	17.8	15.4	15.7
CDM750	19.5	19.2	19.1
SP350	9.5	9.2	9.0
SP550	29.0	27.8	28.1
SP750	38.0	37.0	36.7
MBM350	6.4	4.3	5.9
MBM550	24.2	23.5	23.7
MBM750	17.9	13.2	16.6
CP350	11.0	10.4	10.3
CP550	32.8	31.4	31.9
CP750	41.0	38.8	39.2

4. Conclusions

The CO_2 uptake capacities of chars produced by pyrolysis (350–750 °C) of protein-rich animal wastes (co-digested manure and meat and bone meal) and their representative proteins (soybean protein and collagen) have been analyzed by thermogravimetry and discussed based on char characterization results (elemental analysis, pH, FTIR, XPS and textural properties).

No evidence has been found to indicate that the nitrogenous groups remaining on the char surface after pyrolysis of proteins could favor the adsorption of CO_2, but the theory of volume filling of micropores better explains the mechanism of CO_2 adsorption on this type of chars. This points to the development of an important ultra-microporous structure in protein chars.

Pyrolysis chars from proteins and livestock residues have been proven to adsorb CO_2 reversibly. Protein chars have shown higher CO_2 uptake values than livestock waste chars (up to 20–25 mg CO_2/g char in the case of waste-derived chars and about 40 mg CO_2/g char in the case of protein-derived chars). Although the higher mineral content in the animal waste chars seems to provoke a dilution effect in the CO_2 adsorption capacity, such reduction in the CO_2 adsorption is not as high as expected if considering the ash content, which points to a potential contribution of the ashes to the CO_2 adsorption process, but to a lesser extent than physisorption.

Although CO_2 adsorption capacities of pristine animal waste chars are lower than typical values found for commercial adsorbents, pyrolysis of livestock waste could be a sustainable way to reduce waste generation by producing low-cost co-adsorbents that could be exploited to partially replace the use of other commercial adsorbents, boosting the circular economy in the primary sector.

Future work will be focused on evaluating possible interactions of proteins with other components present in livestock waste, such as cellulose, lignin and mineral fraction, as well as on the effect of other environmental factors, such as the presence of moisture or hydrogen sulfide in biogas, the latter being another impurity to be removed and which could compete with CO_2 adsorption.

CRediT authorship contribution statement

Noemí Gil-Lalaguna: Conceptualization, Formal analysis, Visualization, Writing – original draft, Writing – review & editing. **África Navarro:** Investigation, Data curation, Validation. **Hans-Heinrich Carstensen:** Conceptualization, Investigation, Formal analysis, Writing – review & editing. **Joaquín Ruiz:** Software, Methodology. **Isabel Fonts:** Conceptualization, Methodology, Writing – review & editing. **Jesús Ceamanos:** Resources, Writing – review & editing. **María Benita Murillo:** Resources, Writing – review & editing. **Gloria Gea:** Conceptualization, Methodology, Funding acquisition, Project administration, Supervision, Writing – review & editing.

Declaration of competing interest

The authors declare that they have no known competing financial interests or personal relationships that could have appeared to influence the work reported in this paper.

Acknowledgements

The authors would like to acknowledge the use of the Servicio General de Apoyo a la Investigación- Universidad de Zaragoza. The authors would also like to express their gratitude to the Aragón Government and European Social Fund (Ref. T22-17R) and to *Agencia Estatal de Investigación* in Spain (Project PID2019-107200RB-I00) for financial support. Also thanks for the Grant ***PLEC2021-008086*** funded by MCIN/AEI 10.13039/

501100011033 and by the "European Union NextGenerationEU/PRTR". I. Fonts acknowledges the Agencia Estatal de Investigación, European Social Fund and University of Zaragoza for the post-doctoral contract awarded (RYC2020-030593-I). A. Navarro-Gil acknowledges the Agencia Estatal de Investigación for the pre-doctoral grant received (PRE2020-093382)

References

Angelidaki, I., Treu, L., Tsapekos, P., Luo, G., Campanaro, S., Wenzel, H., Kougias, P.G., 2018. Biogas upgrading and utilization: current status and perspectives. Biotechnol. Adv. 36 (2), 452–466. https://doi.org/10.1016/J.BIOTECHADV.2018.01.011.

Awe, O.W., Zhao, Y., Nzihou, A., Minh, D.P., Lyczko, N., 2017. A review of biogas utilisation, purification and upgrading technologies. Waste Biomass Valoriz. 8 (2), 267–283. https://doi.org/10.1007/S12649-016-9826-4/FIGURES/9.

Cai, S., Zhang, Q., Wang, Z., Hua, S., Ding, D., Cai, T., Zhang, R., 2021. Pyrrolic N-rich biochar without exogenous nitrogen doping as a functional material for bisphenol a removal: performance and mechanism. Appl. Catal. B Environ. 291, 120093. https://doi.org/10.1016/J.APCATB.2021.120093.

Chen, J., Yang, J., Hu, G., Hu, X., Li, Z., Shen, S., Radosz, M., Fan, M., 2016. Enhanced CO2 capture capacity of nitrogen-doped biomass-derived porous carbons. ACS Sustain. Chem. Eng. 4 (3), 1439–1445. https://doi.org/10.1021/ACSSUSCHEMENG.5B01425/ASSET/IMAGES/LARGE/SC-2015-014258_0004.JPEG.

Chen, Y., Zhang, X., Chen, W., Yang, H., Chen, H., 2017. The structure evolution of biochar from biomass pyrolysis and its correlation with gas pollutant adsorption performance. Bioresour. Technol. 246, 101–109. https://doi.org/10.1016/J.BIORTECH.2017.08.138.

Côrtes, L.N., Druzian, S.P., Streit, A.F.M., Godinho, M., Perondi, D., Collazzo, G.C., Oliveira, M.L.S., Cadaval, T.R.S., Dotto, G.L., 2019. Biochars from animal wastes as alternative materials to treat colored effluents containing basic red 9. J. Environ. Chem. Eng. 7 (6), 103446. https://doi.org/10.1016/J.JECE.2019.103446.

Creamer, A.E., Gao, B., Wang, S., 2016. Carbon dioxide capture using various metal oxyhydroxide-biochar composites. Chem. Eng. J. 283, 826–832. https://doi.org/10.1016/j.cej.2015.08.037.

Creamer, A.E., Gao, B., Zhang, M., 2014. Carbon dioxide capture using biochar produced from sugarcane bagasse and hickory wood. Chem. Eng. J. 249, 174–179. https://doi.org/10.1016/J.CEJ.2014.03.105.

Dissanayake, P.D., Choi, S.W., Igalavithana, A.D., Yang, X., Tsang, D.C.W., Wang, C.H., Kua, H.W., Lee, K.B., Ok, Y.S., 2020. Sustainable gasification biochar as a high efficiency adsorbent for CO2 capture: a facile method to designer biochar fabrication. Renew. Sust. Energ. Rev. 124, 109785. https://doi.org/10.1016/J.RSER.2020.109785.

Dissanayake, P.D., You, S., Igalavithana, A.D., Xia, Y., Bhatnagar, A., Gupta, S., Kua, H.W., Kim, S., Kwon, J.H., Tsang, D.C.W., Ok, Y.S., 2020. Biochar-based adsorbents for carbon dioxide capture: a critical review. Renew. Sust. Energ. Rev. 119, 109582. https://doi.org/10.1016/j.rser.2019.109582.

Dubinin, M.M., 1989. Fundamentals of the theory of adsorption in micropores of carbon adsorbents: characteristics of their adsorption properties and microporous structures. Carbon 27 (3), 457–467. https://doi.org/10.1016/0008-6223(89)90078-X.

Hayashi, N., Hayakawa, I., Fujio, Y., 1993. Flow behaviour of soy protein isolate melt with low and intermediate moisture levels at an elevated temperature. J. Food Eng. 18 (1), 1–11. https://doi.org/10.1016/0260-8774(93)90072-R.

Jagiello, J., Kenvin, J., Celzard, A., Fierro, V., 2019. Enhanced resolution of ultra micropore size determination of biochars and activated carbons by dual gas analysis using N2 and CO2 with 2D-NLDFT adsorption models. Carbon 144, 206–215. https://doi.org/10.1016/j.carbon.2018.12.028.

Jiao, Y., Zheng, Y., Smith, S.C., Du, A., Zhu, Z., 2014. Electrocatalytically switchable CO2 capture: first principle computational exploration of carbon nanotubes with pyridinic nitrogen. ChemSusChem 7 (2), 435–441. https://doi.org/10.1002/CSSC.201300624.

Karim Ghani, W.A.W.A., Rebitanim, N.Z., Salleh, M.A.M., Alias, A.B., 2015. Carbon dioxide adsorption on coconut shell biochar. Progress in Clean Energy, Volume 1: Analysis and Modeling, pp. 683–693 https://doi.org/10.1007/978-3-319-16709-1_50.

Lahijani, P., Mohammadi, M., Mohamed, A.R., 2018. Metal incorporated biochar as a potential adsorbent for high capacity CO2 capture at ambient condition. J.CO2 Util. 26, 281–293. https://doi.org/10.1016/J.JCOU.2018.05.018.

Leng, L., Xu, S., Liu, R., Yu, T., Zhuo, X., Leng, S., Xiong, Q., Huang, H., 2020. Nitrogen containing functional groups of biochar: an overview. Bioresour. Technol. 298. https://doi.org/10.1016/J.BIORTECH.2019.122286.

Liang, T., Chen, C., Li, X., Zhang, J., 2016. Popcorn-derived porous carbon for energy storage and CO2 capture. Langmuir 32 (32), 8042–8049. https://doi.org/10.1021/ACS.LANGMUIR.6B01953.

Liu, S.H., Huang, Y.Y., 2018. Valorization of coffee grounds to biochar-derived adsorbents for CO2 adsorption. J. Clean. Prod. 175, 354–360. https://doi.org/10.1016/J.JCLEPRO.2017.12.076.

Madzaki, H., Karimghani, W.A.W.A.B., Nurzalikharebitanim, Azilbaharialias, 2016. Carbon dioxide adsorption on sawdust biochar. Procedia Eng. 148, 718–725. https://doi.org/10.1016/J.PROENG.2016.06.591.

Mulu, E., M'Arimi, M.M., Ramkat, R.C., 2021. A review of recent developments in application of low cost natural materials in purification and upgrade of biogas. Renew. Sust. Energ. Rev. 145, 111081. https://doi.org/10.1016/j.rser.2021.111081.

Pels, J.R., Kapteijn, F., Moulijn, J.A., Zhu, Q., Thomas, K.M., 1995. Evolution of nitrogen functionalities in carbonaceous materials during pyrolysis. Carbon 33 (11), 1641–1653. https://doi.org/10.1016/0008-6223(95)00154-6.

Qiao, Y., Zhang, S., Quan, C., Gao, N., Johnston, C., Wu, C., 2020. One-pot synthesis of digestate-derived biochar for carbon dioxide capture. Fuel 279, 118525. https://doi.org/10.1016/j.fuel.2020.118525.

Rajkovich, S., Enders, A., Hanley, K., Hyland, C., Zimmerman, A.R., Lehmann, J., 2012. Corn growth and nitrogen nutrition after additions of biochars with varying properties to a temperate soil. Biol. Fertil. Soils 48 (3), 271–284. https://doi.org/10.1007/S00374-011-0624-7.

Saha, D., Thorpe, R., van Bramer, S.E., Alexander, N., Hensley, D.K., Orkoulas, G., Chen, J., 2018. Synthesis of nitrogen and sulfur codoped nanoporous carbons from algae: role in CO2 separation. ACS Omega 3 (12), 18592–18602. https://doi.org/10.1021/ACSOMEGA.8B02892/ASSET/IMAGES/LARGE/AO-2018-02892E_0003.JPEG.

Scarlat, N., Fahl, F., Dallemand, J.F., Monforti, F., Motola, V., 2018. A spatial analysis of biogas potential from manure in Europe. Renew. Sust. Energ. Rev. 94, 915–930. https://doi.org/10.1016/J.RSER.2018.06.035.

Sethupathi, S., Zhang, M., Rajapaksha, A.U., Lee, S.R., Nor, N.M., Mohamed, A.R., Al-Wabel, M., Lee, S.S., Ok, Y.S., 2017. Biochars as potential adsorbers of CH4, CO2 and H2S. Sustainability 9 (1), 121. https://doi.org/10.3390/SU9010121.

Stoeckli, H.F., 1990. Microporous carbons and their characterization: the present state of the art. Carbon 28 (1), 1–6. https://doi.org/10.1016/0008-6223(90)90086-E.

Thommes, M., Kaneko, K., Neimark, A.V., Olivier, J.P., Rodriguez-Reinoso, F., Rouquerol, J., Sing, K.S.W., 2015. Physisorption of gases, with special reference to the evaluation of surface area and pore size distribution (IUPAC Technical Report). Pure Appl. Chem. 87 (9–10), 1051–1069. https://doi.org/10.1515/PAC-2014-1117.

Wang, P., Guo, Y., Zhao, C., Yan, J., Lu, P., 2017. Biomass derived wood ash with amine modification for post-combustion CO2 capture. Appl. Energy 201, 34–44. https://doi.org/10.1016/J.APENERGY.2017.05.096.

Wang, Y., Hu, X., Hao, J., Ma, R., Guo, Q., Gao, H., Bai, H., 2019. Nitrogen and oxygen codoped porous carbon with superior CO2 adsorption performance: a combined experimental and DFT calculation study. Ind. Eng. Chem. Res. 58 (29), 13390–13400. https://doi.org/10.1021/ACS.IECR.9B01454/SUPPL_FILE/IE9B01454_SI_001.PDF.

Wedler, C., Span, R., 2021. Micropore analysis of biomass chars by CO2 adsorption: comparison of different analysis methods. Energy Fuel 35 (10), 8799–8806. https://doi.org/10.1021/ACS.ENERGYFUELS.1C00280.

Xiong, Z., Shihong, Z., Haiping, Y., Tao, S., Yingquan, C., Hanping, C., 2013. Influence of NH3/CO2 modification on the characteristic of biochar and the CO2 capture. Bioenergy Res. 6 (4), 1147–1153. https://doi.org/10.1007/S12155-013-9304-9.

Xu, X., Kan, Y., Zhao, L., Cao, X., 2016. Chemical transformation of CO2 during its capture by waste biomass derived biochars. Environ. Pollut. 213, 533–540. https://doi.org/10.1016/J.ENVPOL.2016.03.013.

Yang, Z., Zhang, G., Xu, Y., Zhao, P., 2019. One step N-doping and activation of biomass carbon at low temperature through NaNH2: an effective approach to CO2 adsorbents. J.CO2 Util. 33, 320–329. https://doi.org/10.1016/J.JCOU.2019.06.021.

Zhang, X., Zhang, S., Yang, H., Feng, Y., Chen, Y., Wang, X., Chen, H., 2014. Nitrogen enriched biochar modified by high temperature CO2-ammonia treatment: characterization and adsorption of CO2. Chem. Eng. J. 257, 20–27. https://doi.org/10.1016/J.CEJ.2014.07.024.

Zhang, X., Zhang, S., Yang, H., Shao, J., Chen, Y., Feng, Y., Wang, X., Chen, H., 2015. High temperature ammonia modification of rice husk char to enhance CO2 adsorption: influence of pre-deashing. RSC Adv. 5 (128), 106280–106288. https://doi.org/10.1039/C5RA23365H.

Zhang, X., Wu, J., Yang, H., Shao, J., Wang, X., Chen, Y., Zhang, S., Chen, H., 2016. Preparation of nitrogen-doped microporous modified biochar by high temperature CO2-NH3 treatment for CO2 adsorption: effects of temperature. RSC Adv. 6 (100), 98157–98166. https://doi.org/10.1039/c6ra23748g.